Land Use Policy 61 (2017) 171–184

Contents lists available at ScienceDirect

Land Use Policy

journal homepage: www.elsevier.com/locate/landusepol

Orienting rocky desertification towards sustainable land use: An advanced remote sensing tool to guide the conservation policy

Heyuan You*

School of Public Administration, Zhejiang University of Finance and Economics, Hangzhou, Zhejiang 310018, China

ARTICLE INFO

Article history:
Received 6 September 2016
Received in revised form 24 October 2016
Accepted 1 November 2016
Available online 22 November 2016

Keywords:
Land desertification
Rocky desertification monitoring
Sustainable land use management
Sub-pixel mapping
Spectral unmixing
Ecological restoration project
Land conservation policy

ABSTRACT

Due to non-sustainable land management, desertification has been occurring widely across the world and continues to be a global land use problem. In this context, appropriate methodological tools, which can provide a biased estimation of desertification, are critical for learning from past failures and local successes in orienting desertification towards sustainable land use. This paper proposes a locally adaptive multiple endmember spectral mixture analysis (MESMA) algorithm to extract the rocky desertification information from medium resolution images at subpixel level and applies it to the case of Danjiangkou reservoir region (DRR), China. Quantitative comparisons show that the locally adaptive MESMA has achieved more accurate and reliable estimations of rocky desertification information in DRR than the traditional MESMA. An inversed U-shaped trend is observed for desertified land with different severity levels from 1987 and 2013 in DRR. In particular, the inflection point roughly emerged in period 2000–2005. Casual mechanism-based regressions demonstrate that such dynamics of rocky desertification are closely coupled with socioeconomic, biophysical, and policy factors. More specifically, we identify a significantly positive role of land conservation policy in combating and relieving rocky desertification in DRR. Positive effects are observed particularly through afforestation, investment, and professionals input. Based on the conclusions and lessons of DRR, I finally make relevant recommendations for formulating policies and strategies that attempt to orient desertification towards sustainable land use. The proposed locally adaptive MESMA can act as an advanced remote sensing tool to guide the conservation policy.

1. Introduction

1.1. Desertification: a global land use problem

Central to the food, water, and energy nexus, land has an essential role in securing food productivity, regulating water cycle, maintaining biodiversity, enhancing resilience to climate change, and supporting energy provisioning (Thomas et al., 2012). Due to non-sustainable land management, however, land degradation and its manifestation as desertification in arid, semiarid, and dry sub-humid regions have been occurring widely across the world. Desertification is defined as a persistent loss of ecosystem function and productivity due to diverse disturbances (e.g., soil fertility loss, soil erosion, vegetation cover loss, and plant species changes) from which the land cannot unaided recover (Bai et al., 2008; Safriel and Adeel, 2005). Global desertified land covers approximately 41% of the total terrestrial surface and affects more than two billion population (MEA, 2005), including Africa (Kiage, 2013), America (Vieira et al., 2015), Asia (Miao et al., 2015), Europe (Salvati and Bajocco, 2011), and Oceania (Williams, 2015). The figure is expected to increase substantially against the population growth and climate change (Reynolds et al., 2007; UNCCD, 2008). Desertification jeopardizes and disfunctions the biophysical and socioeconomic processes, making it among the most challenging environmental problems of the 21 st century (MEA, 2005; Reynolds et al., 2007; Vogt et al., 2011).

Past decades have seen great efforts to initialize national and international policies to combat desertification. Though more than 190 countries have acted actively, no substantial progress has been achieved towards controlling the desertification for the entire world. Vigorous scientific debate remains with respect to the measurement and causes of desertification, let alone the best mitigation solution. Existing thematic maps at global level are generally based on coarse resolution data and simply indicate the vulnerability to desertification, such as the USDA NRCS Desertification Vulnerability map (Eswaran and Reich, 2003), GLASOD (Thomas and Middleton, 1994), the United Nations World Atlas of Desertification

* Corresponding author at: No.18 Xueyuan Street, Area Code: 310018, Hangzhou, Zhejiang Province, China.
E-mail address: youheyuan@zufe.edu.cn

http://dx.doi.org/10.1016/j.landusepol.2016.11.024
0264-8377/

(UNEP, 1997), the Millennium Ecosystem Assessment Desertification Synthesis (MEA, 2005), as well as those produced individually by Ramankutty and Foley (1999), Lepers et al. (2005), Campbell et al. (2008), and Cai et al. (2011). Moreover, these thematic maps differ in standard, accuracy, and consistence (Gibbs and Salmon, 2015; Vogt et al., 2011). It leads to the dilemma that there lacks of robust, spatially explicit, and producible methodologies and no formal indicators or benchmarks are available for monitoring the progress in combating desertification.

Since desertification continues to be a global land use problem, it requires urgently to develop robust and practical tools to capture the extent and severity of desertification. As such, the worldwide political discussions can formulate more efficient mitigation and adaption to desertification. Indeed, desertification is resulted from a number of biophysical processes and their complex interactions with multi-level anthropologic drivers, ranging from individual household level, whose land use practices are spontaneous but may be negligent and exploitative, to land use policy level at which land management strategies are planned but can be economy-oriented and discriminatory (Bai et al., 2008; Gao and Liu, 2010; Geist and Lambin, 2004; Nkonya et al., 2011; von Braun et al., 2012; Vu et al., 2014a). In several instances, individual households and policy makers have implemented sustainable land use practices and policies, which have prevented and slowed further degradation (Fleskens and Stringer, 2014). These isolated success stories are regarded to have great value as international references (Fleskens and Stringer, 2014). Scholars thus argue that we should move towards upscaled sustainable land use for addressing global challenges in the post-2015 era. In this context, appropriate methodological tools, which can provide a biased estimation of desertification, are critical for learning from past failures and local successes in orienting desertification towards sustainable land use.

1.2. China's desertification and policy responses

China is one of the most vulnerable countries to desertification in the world. Almost all semi-arid, arid, and sub-humid regions are attracted by desertification in China (Yan and Cai, 2015). It is roughly estimated that over 200 million population and 16 million km^2 areas are susceptible to desertification (Wang et al., 2008). Desertification presents different characteristics across the Chinese vast territory (Zhu and Wang, 1993). In the northern China, aeolian desertification resulted from wind erosion is the dominant process of desertification. Aeolian desertified land increased at a rate of 1560 km^2y^{-1} in period 1955–1975, 2100 km^2y^{-1} in period 1976–1987, and 3600 km^2y^{-1} in period 1988–2000 (Wang et al., 2004a, 2004b). Water and soil loss, resulting from irrational use of sloping land (e.g., Loess Plateau), is the principle process of desertification in the northwest plateau (Zhao et al., 2015). The desertified land suffering from soil erosion amounts to 45.4×10^4 km^2, accounting for 71% of the total area of Loess Plateau. Salinization caused by unsustainable management and irrigation acts as the primary process of desertification in the north plain, northwest inland, and coastal areas. Rocky desertification due to intensive anthropogenic activities on ecologically fragile karst formations colonizes the seven provinces (Chongqing, Hubei, Hunan, Guangdong, Guangxi, Guizhou, Sichuan, and Yunnan) in southwest China. It is estimated that 5.8% of the total land in southwest China are covered by exposed or outcropped carbonate rock areas and the rocky desertified land reaches 13.0×10^4 km^2 in 2005 (Yan and Cai, 2015). With the respect to the extent and severity, desertification in the southwestern, northeastern, and central zones is more serious than that in the northwest (Yan and Cai, 2015). As for the increasing trend, southwest and northeast are the hotspots of the newly desertified land (Yan and Cai, 2015). Desertification has posed great threat to China's environmental sustainability, socioeconomic development, and human well-being. Unfortunately, no reliable and unified data are available for long time-series and cross-regional comparisons. The trend and magnitude of desertification remain unclear in China. It therefore requires efficient tools to capture the desertification dynamics with high accurate estimations.

The Chinese government has set high priorities on agenda to combat desertification. Since the 1980s, a series of programs and policies have been launched to rehabilitate desertified land (Sun, 2015). The 'Three North' project of the agropastoral zone, titled as the Green Great Wall, has achieved 4069 million km^2 afforested area in northern China (Zha and Gao, 1997). To address the desertification in northwest China, the 'Grain for Green' program has been implemented, which calls for the conversion of farmland to forest on sloping land. The National Reform and Development Commission has carried out a number of ecological restoration projects to rehabilitate the karst desertified land in southwest China. These projects cover 100 counties, accounting for over 97% of total counties in southwest China (SFA, 2004). Scientific and political communities have acknowledged the role of these policies and programs in releasing desertification. As a consequence of policies and project-based initiatives, for example, desertification reversal has occurred in some parts of in the agropastoral zones (Gerile and Wulantuya, 2004; Jiang et al., 2014; Piao et al., 2005; Qi et al., 2012; Xue et al., 2005; Zhao et al., 2010; Zhou et al., 2012). It is reported that more than 70% of the most severe karst desertified surfaces have been rehabilitated. However, the central government has put overwhelming emphasis on the northwestern zones (e.g., Loess Plateau), and the central, southwestern, and northeastern zones are somewhat neglected. The extent and severity of desertification still expand in many regions, such as the Liao River watershed in the northeast, the middle part of Yellow River basin in the central China, the middle part of Yangtze River basin in the southwest, and the Pearl River watershed in the south (Jiang et al., 2014). The Chinese government still has to accomplish tremendous tasks for preventing further desertification. The lessons and successes of China's policy responses to desertification will be very helpful for global sustainable land use practice.

1.3. Present study

The present study focuses on the rocky desertification, the process of which the original vegetated karst surfaces transform into a non-vegetated landscape characterized by bare soils and rocks (Yuan, 1997). Rocky desertification is primarily observed in southwest China (Yuan, 1997), the Dinaric Karst (Gams and Gabrovec, 1999), and the European Mediterranean basin (Yassoglou, 2000). In addition, rocky desertification also occurs typically in the Gunung Sewu of Indonesia (Sunkar, 2008), Ryukyu Islands of Japan (Ford and Williams, 2007), Israel, Mexico, Guatemala, and Belize. In southwest China, more specifically, area exposed to carbonate rock amount to 50.6×10^4 km^2 (26.0% of the total area), and rocky desertified land reach 11.4×10^4 km^2 in 2000 (5.8% of the total area) (Jiang et al., 2014). Rock desertification in southwest China is primarily distributed in the Yangtze River Southwest drainage basin, the Transboundary River basin, and the Pearl River basin (Li et al., 2009; Bai et al., 2013). The present study explores one typical region in the Yangtze River Southwest drainage basin as the case—the Danjiangkou reservoir region (DRR). The DRR sits at the Qinli-Bashan Mountain region in northwest Hubei Province (Fig. 1) and is featured by sub-tropic karst landscapes. The DRR has a monsoon continental semi-humid climate with plenty rainfall and four distinctive seasons. Annual average temperature is 14.1–15.7 °C and annual average precipitation amounts to 800–1000 mm. Topography within the DRR is complicated and varied, with plains basins, mountains, and hills. The DRR is the water source for the mid-

Fig. 1. Location of the Danjiangkou reservoir region, China.

dle route of South-to-North Water Transfer Project in China. In this regard, the eco-environmental quality is extremely important for China's water security and sustainability. However, the severe rocky desertification has gradually deteriorated the water environment and thus become a bottleneck problem for implementing the South-to-North Water Transfer Project. In order to combat the rocky desertification, the Chinese central government has launched a number of pilot ecological restoration projects in the DRR. In response, the local government formulated the land conservation policy in 2000, which regulates seven major countermeasures to rocky desertification: (1) artificial afforestation and sealing off mountainous areas for restoration; (2) education campaigns to promote environmental awareness and encourage public participation; (3) scientific and systematic project engineering planning; (4) cross-sectional cooperation; (5) afforestation subsidy and confirmation of forested land use right; (6) providing technological support and expanding the application of advanced new techniques; (7) formulation of regulations to supervise the rocky desertification activities. The lessons learnt from the DRR should provide essential international inferences to achieve sustainable land use practice. It therefore requires to develop robust tools for investigating the dynamic extent and severity of rocky desertification in DRR and evaluating the role of land conservation policy. I specifically attempt to: (1) develop a remote sensing tool to reliably and accurately extract the rocky desertification information; (2) monitor the dynamic extent and severity of rocky desertification in DRR; (3) quantify the role of land conservation policy in combating the rocky desertification; and (4) fuse insights into sustainable land use that can be applicable across a range of international settings.

The remainder of this paper is organized as follows: (1) Section 2 reviews three issues of desertification relevant literature: conceptualizations, methodological tools for monitoring and assessment, and policy responses; (2) Section 3 describes the study area, and introduces the proposed methodology for rocky desertification measurement; (3) Section 4 discusses the main findings and provides some implications for sustainable land use practices.

2. Literature review

2.1. Conceptualizations

Desertification, first introduced by Aubréville (1949), is subjected to a variety of definitions. Original definitions in the 1980s from different perspectives are reviewed by Glantz and Orlovsky (1983) and Verstraete (1986). Since the 1990s, conceptualizations have gradually evolved from a simple climatically driven concept (Aubréville, 1949) to a complex cognition on productive potential for human society (e.g. ELD Initiative, 2013; Kasperson et al., 1995; UNEP, 1997) and biophysical functions and services (e.g. Dean et al., 1995; IPCC, 2001). For details of the conceptualization evolution, see Herrmann and Hutchinson (2005) for a review. According to international agreement, the most authoritative one is defined by the UNCCD as 'the climate and human driven land degradation in semiarid, arid, and dry subhumid regions' (UNCCD, 1995). However, much room is left for interpreting this definition and ambiguities emerge as a consequence. There still lacks of clear explanations on what desertification is and how to quantify it (Grainger, 2009). As for the rocky desertification, the Chinese government defines it as: the land degradation in tropical and subtropical karst regions driven by the human activities and humid and semi-humid climate, and is characterized by severe soil erosion, deteriorated vegetation cover, widespread exposed bedrock, and rock stacking.

2.2. Methodologies of desertification monitoring and assessment

Field survey and remote sensing are the two principle approaches to desertified land quantification. Compared with field survey, remote sensing tools are more time-efficient and cost-effective and are thus more frequently applied to monitor and assess desertification. With respect to the data sources, diverse multispectral and hyperspectral sensors have been utilized with wide spectrum of resolutions (e.g., MODIS, Landsat, EO-1 Hyperion, aerial photographs). Medium resolution data, the Landsat imageries in particular, have been widely used, given their suitable geographic coverage, high temporal resolution, and free accessibility. The Landsat imageries are therefore acknowledged as feasible and promising data sources for documenting regional and global desertification dynamics. With respect to the methodology, the major remote sensing tools can be categorized into four broad streams: (1) visual interpretation based on expert opinion; (2) satellite derived ecological indicators; (3) assimilation with biophysical models; (4) machine-based supervised classification.

Visual interpretation based on expert opinion is the first approach employed to quantify and map desertified land around the world and maintains as a mainstay until today (Nijsen et al., 2012). Based on the structural elements (e.g., pattern, size, texture) and color-composited features, the experienced interpreters recognize the desertified surfaces (Campbell, 2002) and distinguish them against noises (Bruce et al., 2003). Visual interpretation generally produce high accuracy in mapping desertification (Achard et al., 2002; Bot et al., 2000; FAO, 2001), but it is also subjected to subjectivity, inconsistence, and increased omission risk. It is particularly difficult to overcome these inevitable limitations, given the lacking of precise definitions and severity classifications for desertification. The leading role of expert opinion approach would be decreased on condition that accurate information of soil and vegetation can be extracted by the other approaches.

Vegetation cover loss, soil erosion, and declined biomass productivity are the most observable consequences of desertification. As a result, scholars are fancy of using satellite derived ecological indicators to distinguish the desertified land surfaces, such as the vegetation indices, soil spectral properties, and landscape fragmentation (Hartia et al., 2016; Lamchin et al., 2016; Pan and Qin, 2010; Su et al., 2014; Vägen et al., 2013; Wu et al., 2010; Xiao et al., 2006). Among these indicators, the Normalized Difference Vegetation Index (NDVI) is the most widely applied one (Bai et al., 2008; Bastin et al., 1995; Wessels et al., 2012). Researchers typically refer to NDVI time series data to capture the desertification potentials. However, the satellite derived ecological indicators can only depict the surfaces potentially affected by desertification, but cannot capture the actual picture of the desertified land. Some scholars attempt to assimilate remote sensing data with biophysical models to quantify the desertification, such as the vegetation productivity model, vegetation growth model, soil erosion model, energy balance and evapotranspiration models (García et al., 2008; Prince et al., 2009; Saygın et al., 2011; Symeonakis and Drake, 2004; Vu et al., 2014b). The biophysical modeling assimilated with remote sensing data approach show promising potential to reliably map desertified land. Unfortunately, biophysical models require large quantities of observation and calibration data, and is very sensitive to data quality and inherent error. The capability to yield large scale desertification information is rather limited.

The machine-based supervised classification offers a major opportunity to improve the spatial representation of desertified lands in a consistent, easy and accurate manner. Methods are emerging that attempt to quantify desertification severity and extent, including maximum likelihood algorithm (Huang and Cai, 2009), band combination and calculation (Chen et al., 2003; Yue et al., 2011), object-based mapping (Xiong et al., 2008), and support vector machine (Xu et al., 2015). The mentioned methods extract the desertification information at pixel level and generate classification results with relatively lower accuracy, given the large amount of mixed pixels due to high spectral heterogeneity. Some scholars employ the spectral unmixing tools to map the desertification at sub-pixel level (Hill et al., 1995; Dawelbait and Morari, 2012; Tromp and Epema, 1999; Zhang et al., 2014). However, prior studies extensively unmix the pixels with fixed endmembers in a linear manner. Such operation prevents generating satisfactory accuracy of desertification mapping in large areas. It is thus argued that more advanced supervised algorithm should be developed to achieve sub-pixel desertification mapping with high accuracy.

2.3. Policy responses to desertification

Before the adoption of United Nations Convention to Combat Desertification (UNCCD) in 1994, several nations initialized policies for controlling soil erosion, including the Sri Lanka (Joachim and Pandithasekera, 1930), Malawi, Zambia, and Zimbabwe (Jackson, 1960), Brazil (Lal, 1977), and USA (Trimble, 1985). A number of international projects were also launched, such as the United Nations Conference on Desertification in 1977, the Provisional Methodology for Soil Degradation Assessment (FAO, 1979), and the United Nations Conference on Environment and Development (UNCED) in 1992. Since the 1994, the United Nations have made periodical calls to combat desertification worldwide, such as the National Plans of Action in the United Nations Convention to Combat Desertification (UNCCD, 1994), the International Year of the Desert and Desertification in 2006, and the global goal of maintaining zero net land degradation in the United Nations Conference on Sustainable Development (UNCCD, 2008). Following this topic, the World Summit on Sustainable Development (WSSD) in 2002 reaffirmed the desertification as a new focal area. The Spanish Ministry of Agriculture, Food, and Environment made the action plan and establish the desertification landscapes within the Spain (MAGRAMA, 2008). Swaziland developed the National Action Programme, which allows for formulating the most appropriate strategies for each county to combat desertification (Stringer, 2009). Vietnam National Action Programme to Combat Desertification launched a series of national policies to promote the forest

cover recovery in the upland and mountain areas (NAP, 2002; Vu et al., 2014a). Nations in central Asia implemented the international programmes such as the Central Asian Countries Initiative for Land Management (Pender and Mirzabaev, 2008) and the Pilot Program for Climate Resilience (Wolfgramm et al., 2011) that advocate the sustainable land use management to combat desertification. The National Reform and Development Commission of China as mentioned before had also initialized different policies and programs to address the desertification in different regions. Though former literature has introduced a great many national and international policy responses to desertification, the performances and roles of these policies were generally discussed based on qualitative descriptions. Rather few studies have examined the role of policies in addressing desertification using quantitative measurements.

3. Data and methodology

3.1. Remotely sensed data and pre-processing

Landsat and CBERS (China-Brazil Earth Resources Satellite) images are selected as the data sources, given their free availability, representativeness of moderate resolution satellite images, and wide applicability in global land cover mapping (Liu et al., 2016; Su et al., 2014; Xiao et al., 2015). Two Landsat and CBERS scenes are needed to cover the entire DRR. Seasons from late spring and early autumn (May–October) represent the phenological growth periods in DRR. Available images are therefore chosen to cover the relevant periods from 1987 to 2013 (Appendix A). The parts of these images covering the DRR are cloud-free. In order to ensure the comparability in subpixel accuracy, all the images are geometrically registered using the second-order polynomial rectification algorithm and control points extracted from topographic map of 1: 50,000 scale. Then, the nearest-neighbor interpolation method is applied to resample all the pixels into 30 m × 30 m. In order to ensure the spectral comparability, all the images are subjected to atmospheric correction using the FLAASH tool in ENVI. Surface reflectance normalization is further applied. More specifically, the images in 2013 are used as reference and all the other images are matched to them in radiometric values using the pseudo-invariant feature regression. Such operation can reduce the influences of phenology and illumination among time-series images. Finally, neighboring scenes within same seasons and years are mosaicked.

3.2. Sub-pixel extraction of rocky desertification

3.2.1. Background: traditional linear spectral unmixing

Spectral unmixing is the most popular technique for decomposing the pixels in remotely sensed imageries into fractions of different endmembers (pure spectra). The predominant advantage of spectral unmixing is that it allows for the variations in both illumination and composition based on the entire set of spectral characteristics instead of limited number of bands (Dennison and Roberts, 2003). Traditionally, spectral unmixing uses the same number of endmembers and assumes a linear combination of the endmembers for an entire image (Su et al., 2011). It receives the criticism for the failure of incorporation of within-class spectral variability and the spectral variability associated with different classes (Roberts et al., 1998; Somers et al., 2011). Scholars have proposed different alternations to address the endmember variability issue, including the multiple endmember spectral mixture analysis (MESMA; Roberts et al., 1998), Bayesian spectral mixture analysis (Song, 2005), and fuzzy un-mixing (Asner and Lobell, 2000). See Somers et al. (2011) for a review. Among these approaches, the MESMA has been successfully applied over a wide spectrum of imageries (Somers et al., 2011), since it recognizes the limits in spectral dimensionality at pixel level and considers the spectral variability across the scene.

Under the MESMA framework, a number of models with different combinations of endmembers are first run for a pixel, and then the most appropriate one with the best fit to the selection criteria is determined. Endmembers used in spectral unmixing can be primarily obtained from two sources: the images pixels themselves, and the spectral library that is collected from laboratory, field trip, high resolution images, or radiative transfer models (Franke et al., 2009). In particular, the image endmembers have more advantage in that (1) they are closely associated with image features (Rashed et al., 2003); and (2) they present canopy-scale rather than leaf-scale spectra, and thus incorporate the non-linear mixing effects. However, selecting the most representative image endmembers is a quite subjective process. Scholars have developed several algorithms to extract the image endmembers automatically such as the sequential maximum angle convex cone algorithm (Zhang et al., 2014), the endmember bundle method (Somers et al., 2012), the intelligent method (Bateson et al., 2000), the piece-wise convex method (Zare and Gader, 2010). These algorithms treat the entire scene as a whole to distinguish the pure endmembers and ignore the local heterogeneity (Deng and Wu, 2013). Consequently, the within-class variability may be largely increased. Actually, the spectral reflectance presents spatial autocorrelated characteristics across pixels in a scene (Shi and Wang, 2014). The spatial autocorrelation offers the opportunity to define local neighborhoods to select the endmembers across the entire image (Deng and Wu, 2013; Ma et al., 2014), reducing the within-class variability, and enhancing the accuracy. In light of this, we propose a locally adaptive MESMA algorithm for sub-pixel mapping rocky desertification.

3.2.2. Proposed algorithm: locally adaptive MESMA

It is a prerequisite to determine the endmembers accurately for unmixing. In reference to the first law of geography, a locally adaptive approach is proposed to determine the endmembers considering the spatial heterogeneity and autocorrelation. Fig. 2 shows the entire workflow of the proposed method. Pixels have their own endmembers, which are extracted from a neighborhood around one pixel. Different from previous studies that empirically choose the appropriate window size of the neighborhood, we employ the semivariogram to determine the spatial range of autocorrelation (Su et al., 2012). The distance threshold within which spatial dependency achieves is selected as the window size of the neighborhood (35 × 35 pixel). To identify the endmembers, a decision tree classifier, using the biophysical composition index (BCI), the normalized difference vegetation index (NVBI), the normalized difference built-up index (NDBI), and the normalized difference water index (NDWI), is first constructed and then a filter with 3 × 3 pixel window size is applied. On condition that all the pixels within the neighborhood are classified as the same class, these homogeneous pixels are regarded to be endmembers. In particular, endmembers in our study include four types: vegetation, bedrock (bare soils), impervious surface, and water. According to the first law of geography, spectral signature of a certain pixel is more similar to that of the nearer endmembers. I therefore assign a distance-based weight for the endmembers in the neighborhood for a certain pixel, with lower weight for the father endmembers and greater weight for nearer endmembers. More specifically, weights are calculated using a Gaussian distance decay function (Eq. (1)). Then, the endmember spectral signature is synthesized based on the weights using the following equation (Eqs. (2) and (3)). During the mixing process, the types and number of endmembers are adaptively determined. For example, the number of endmembers depends on those emerge in the neighborhood. Finally, the fractions of different

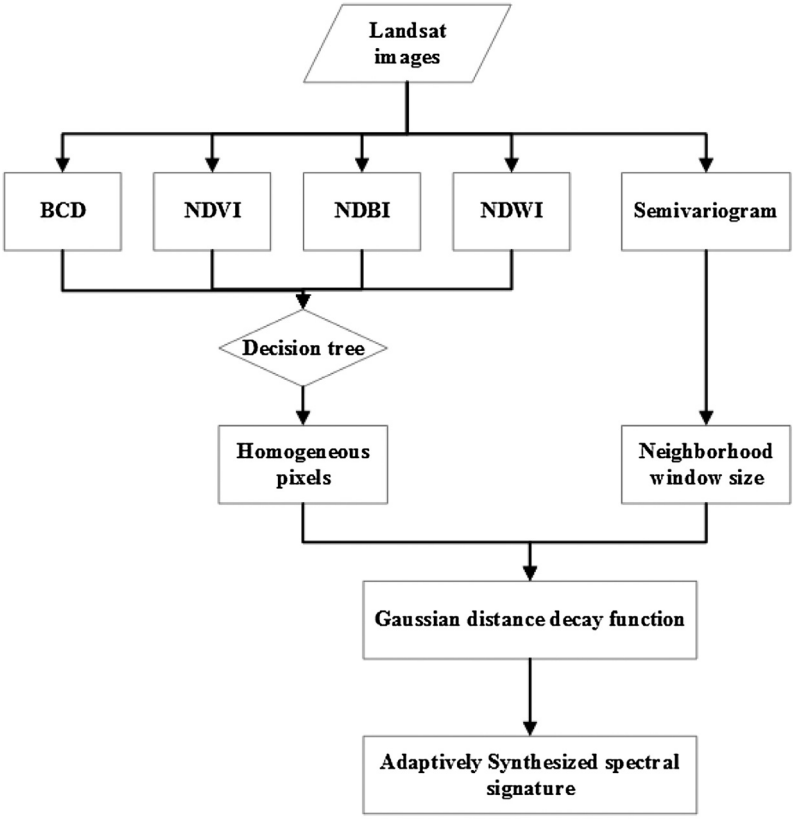

Fig. 2. Workflow chart for the proposed locally adaptive MESMA.

land covers are estimated by a linear MESMA with full abundance constraints (Eqs. (4) and (5)).

$$w_{ij} = \exp(-d_{ij}^2/h^2) \tag{1}$$

where w_{ij} is the weight for endmember j in the neighborhood of pixel i and d_{ij} represents the distance between them; h represents the window size of the neighborhood.

$$r = \sum_{x=1}^{n} \tilde{w}_{ij} r_{ijx} \tag{2}$$

$$\tilde{w}_{ij} = \frac{w_{ijx}}{\sum_{x=1}^{n} w_{ijx}} \tag{3}$$

where n is the number of pixels for one class within the neighborhood, and r_{ijx} is the synthesized signature.

$$R_m = \sum_{i=1}^{n} g_i R_{i,m} + e_m \tag{4}$$

subject to

$$\sum_{i=1}^{n} g_i = 1 \cap g_i > 0 \tag{5}$$

where R_m is the spectral signature of band m; g_i is the fraction of endmember i; n is the number of endmembers; $R_{i,m}$ is the synthesized signature of band m for endmember i; e_m is the error.

3.2.3. Accuracy assessment

I first digitize 120 rectangular samples on high resolution images and aerial photographs for each year and sum the fractions of different land cover types. More specifically, the samples are randomly selected with the size of 90 m × 90 m, in order to reduce the geometric error associated uncertainties between multi-source images (Deng and Wu, 2013). Two error measurements, the root mean square error (RMSE; Eq. (6)) and the correlation coefficient (R^2; Eq. (7)), are then used to assess the accuracy of locally adaptive MESMA. In order to compare the performances of the locally adaptive MESMA and the traditional MESMA, I also implement the traditional MESMA and further apply the T test with 95% confidence to statistically compare their RMSE and R^2.

$$RMSE = \sqrt{\frac{\sum_{i=1}^{n} (\hat{X}_i - X_i)^2}{n}} \tag{6}$$

$$R^2 = \frac{\sum_{i=1}^{n} (\hat{X}_i - \bar{X})}{\sum_{i=1}^{n} (X_i - \bar{X})^2} \tag{7}$$

3.3. Spatial analysis

According to the official standard of Hubei Province that is made by the local government, the severity of rocky desertification is classified into five categories in DRR (Appendix B). Following the standard, I import the interpreted fraction maps into a GIS (geographic information system) and convert the pixels into corresponding rocky desertification severity categories. I then sum the area of rocky desertified land with different severity levels. The thematic maps are further overlaid with a digital elevation model (1: 50,000), in order to analyze the spatial distribution of rocky deser-

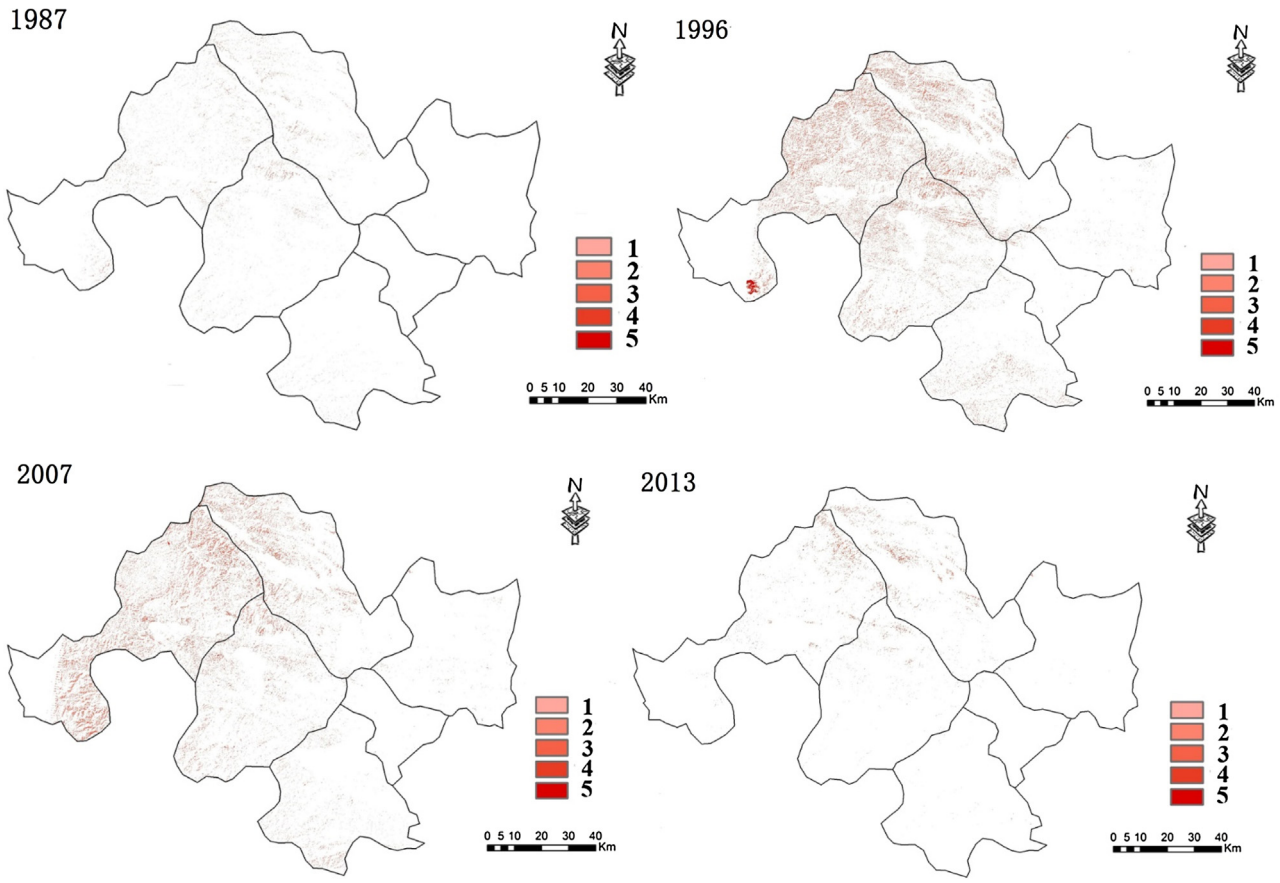

Fig. 3. Rocky desertification information extracted by the locally adaptive MESMA in Danjiangkou reservoir region, China.

tification. More specifically, I sum the area of rocky desertified land associated with elevation and slope gradients.

3.4. Regression analysis

General determinants of land degradation and desertification can be categorized into four principle domains: demographic, policy and institutional, socioeconomic, and biophysical (Dimobe et al., 2015; Geist and Lambin, 2004; Nkonya et al., 2011; Vlek et al., 2008; Vu et al., 2014a; Xu et al., 2013). I therefore establish the casual mechanism-based regression to quantify the role of land conservation policy. The casual mechanism-based regression is based on the well-known mechanism that governs the land desertification, including demography, socioeconomics, biophysical characteristics and policy. More specifically, the land conservation policy is measured by four variables: afforestation area, involved scientific and technological staff, total investment, and implementation temporal duration. These four variables indicate the major countermeasures adopted to combat rocky desertification in DRR. Other exploratory variables include population density, road total length, household income, gross domestic product, average slope of non-desertified land, average elevation of non-desertified land, and proportion of different soil types of the non-desertified land (limestone and lithosol). These variables represent the demographic, socioeconomic, and biophysical conditions of the DRR. Original data for the variables are provided by the local governments. Misleading estimations can be resulted from high multi-collinearity among explanatory variables (Liu et al., 2016; Su et al., 2016; Wan and Su, 2016; You, 2016). Variance inflation factors (VIF) and tolerance values (TV) are used to test the multi-collinearity among explanatory variables before the regression. The criteria for multi-collinearity are VIF >5 and TV < 0.2. In addition, a series of regressions are built

Table 1
Performances of the traditional and locally adaptive multiple endmember spectral mixture analysis.

Year	RMSE		R^2	
	Traditional	Locally adaptive	Traditional	Locally adaptive
1987	0.18	0.13	0.70	0.78
1996	0.16	0.12	0.74	0.81
2001	0.17	0.12	0.73	0.79
2002	0.15	0.11	0.75	0.82
2004	0.17	0.11	0.71	0.84
2007	0.16	0.10	0.74	0.80
2008	0.14	0.11	0.71	0.79
2010	0.17	0.12	0.73	0.83
2011	0.15	0.10	0.74	0.81
2013	0.17	0.12	0.73	0.84
T-test	Mean difference = 0.048 (p = 0.000)		Mean difference = −0.083 (p = 0.000)	

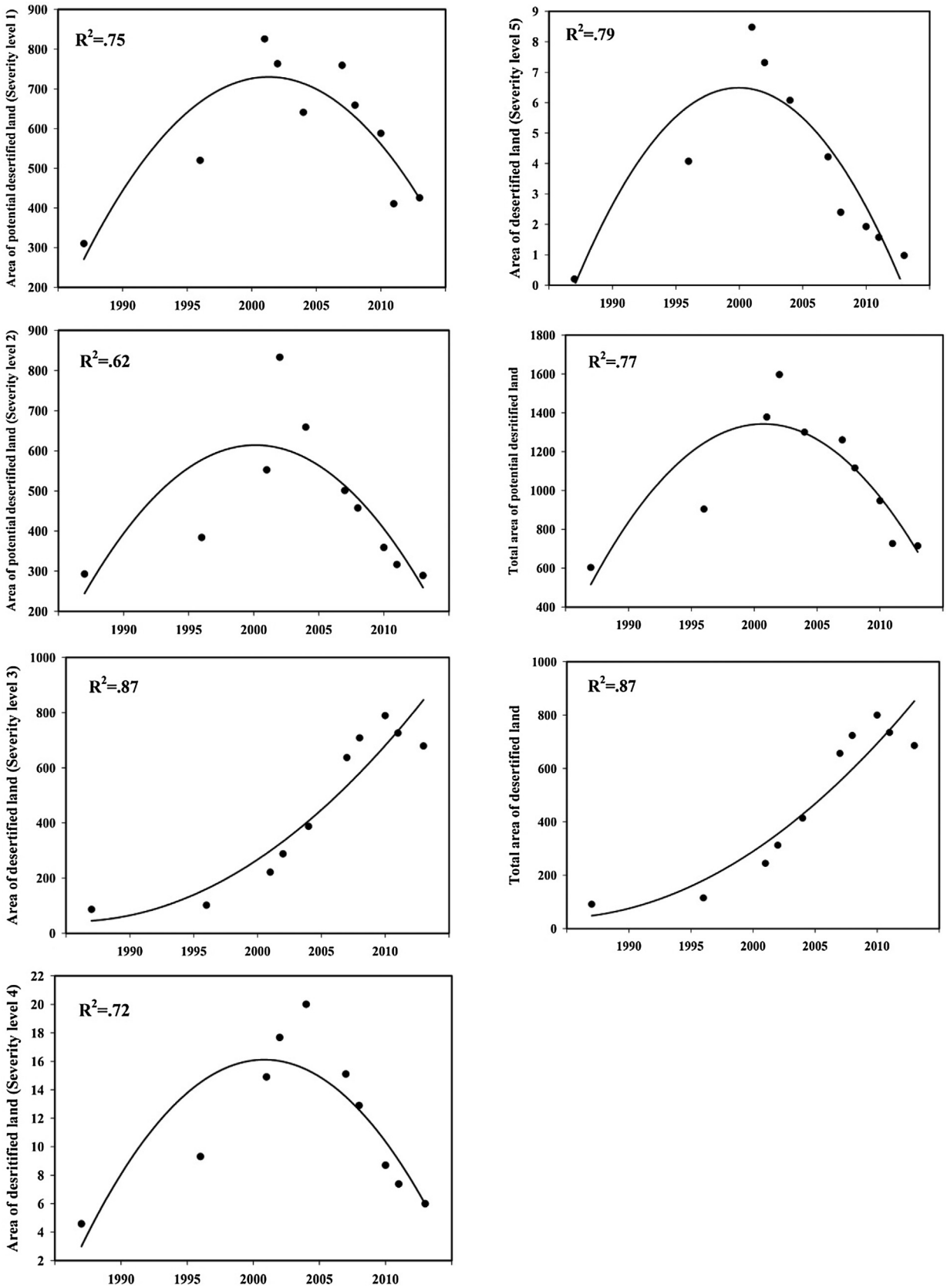

Fig. 4. Temporal trend of desertified land of different severity levels from 1987 to 2013 in the Danjiangkou reservoir region, China (unit: ha).

for total area of rocky desertified land and that of different severity levels.

4. Results

4.1. Algorithm performances

Fig. 3 shows the rocky desertification information extracted by the locally adaptive MESMA. Table 1 summarizes the performances of the locally adaptive MESMA and traditional MESMA. For the locally adaptive MESMA, the RMSE ranges from 0.10 to 0.13 and the R^2 ranges from 0.78 to 0.84. RMSEs of the locally adaptive MESMA are lower than those of the traditional MESMA. Conversely, the R^2 of the locally adaptive MESMA are higher than those of the traditional MESMA. These results demonstrate that the performance of locally adaptive MESMA is better than that of traditional MESMA. The *T*-test confirms that the superiority of locally adaptive MESMA is of statistical significance. It suggests that the locally adaptive MESMA is more capable to extract the rocky desertification information.

4.2. Dynamic extent and severity of rocky desertification

The temporal trend of desertified land with different severity levels is shown in Fig. 4. An inversed U-shaped trend is generally observed for the areal changes of desertified land with different severity levels from 1987 and 2013 in DRR. More specifically, the area of potential desertified land (severity 1, 2, and total) and area of desertified land (severity 4 and 5) first increased rapidly and then decreased gradually around period 2000–2005. The inflection point roughly coincides with the start time of the land conservation policy in 2000. Differently, area of desertified land (severity 3 and total) apparently began to decrease in 2008 but did not statistically exhibit inflection point. Distribution of desertified land associated with topology gradients is presented in Fig. 5 (slope) and Fig. 6 (elevation). It can be seen that desertified and potential desertified land mainly locate in areas with gentle slope (15–25°). Except for the low elevation zone (<100 m), no obvious differences are identified for the other elevation zones. Such results suggest that desertification are more likely to occur in areas with steep slope.

4.3. Role of the land conservation policy

Table 2 demonstrates the outputs of the casual mechanism-based regression. Among the variables of land conservation policy, area of potential desertified land negatively associates with the involved scientific and technological staff (severity level 1) and total investment (severity level 2 and total area), while area of desertified land negatively correlates with the afforestation area (severity level 3, 4, 5 and total), total investment (severity level 3 and 4), and implementation temporal duration (severity level 3 and total). It suggests that the land conservation policy can significantly combat the rocky desertification in DRR. Among the socioeconomic variables, road total length positively accounts for area of potential desertified land (severity level 2), while household income acts as negative exploratory factor for total area of potential desertified land, area of desertified land (severity level 3), and total area of desertified land. Among the biophysical variables, average slope of non-desertified land (SLOPE) is a positive exploratory variable, while proportion of non-desertified land with lithosol soil type (LITH) is a negative exploratory factor. It indicates that rocky desertification is more likely to occur in areas with relatively steep slope.

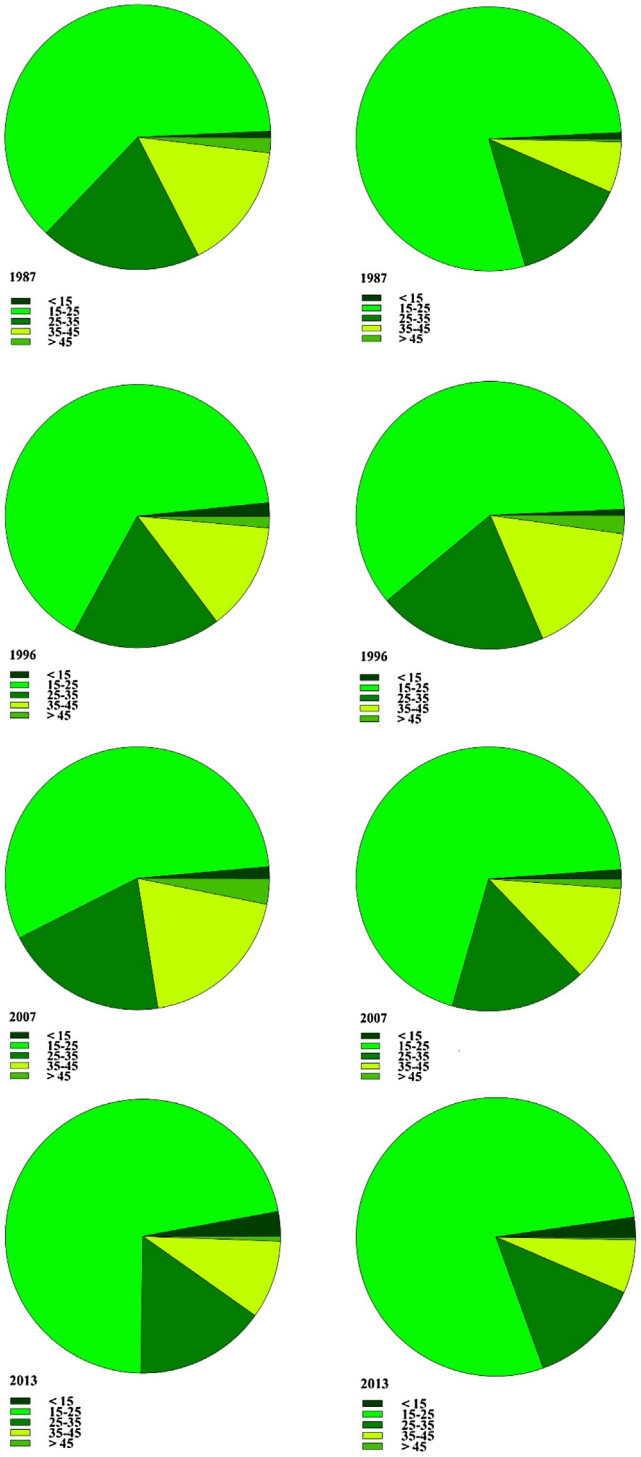

Fig. 5. Distribution of total potential desertified land (left column) and total desertified land (right column) in different slope zones (unit: °).

5. Discussion

Rocky desertification is a highly complex phenomenon both in spatial and temporal dimensions, whist the in-field trips are laborious, expensive and incapable to capture the dynamic process across time and space. In order to formulate conservation policy for mitigation, it is therefore urgent to develop effective methods for mapping rocky desertification based on the remotely sensed imageries. In particular, the medium resolution images, featured by suitable geographic coverage, high temporal resolution,

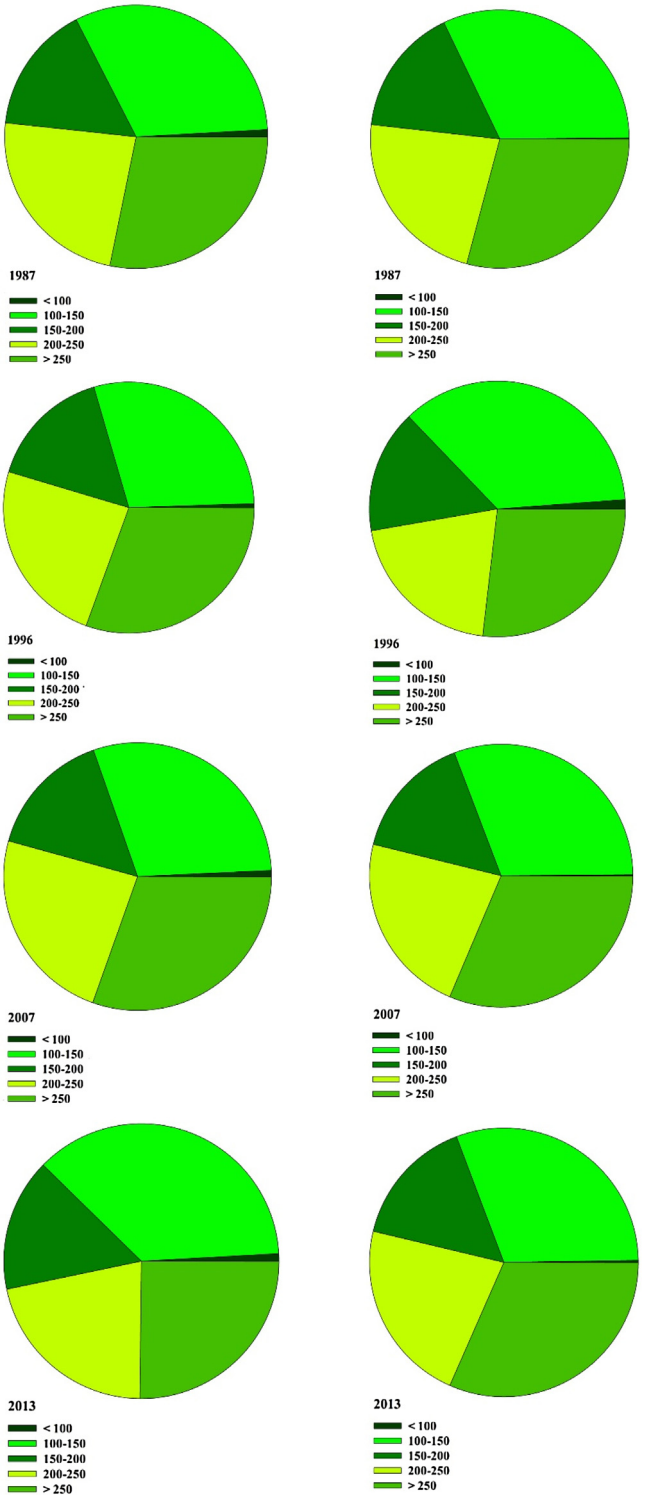

Fig. 6. Distribution of total potential desertified land (left column) and total desertified land (right column) in different elevation zones (unit: m).

and free accessibility, are the most appropriate data sources for producing thematic maps of the extent and hotspots of rocky desertification. Based on such spatially explicit maps, policy makers can make more locally targeted land use management recommendations. This paper proposes a locally adaptive MESMA algorithm to extract the rocky desertification information from medium resolution images at subpixel level. From a methodological standpoint, the locally adaptive MESMA shows significant superiority in addressing endmember spectral heterogeneity. More specifically, the locally adaptive MESMA advances the traditional MESMA in three major aspects: (1) it selects the endmembers within a local neighborhood rather than from a global spectral library; (2) it uses synthetic endmember signatures rather than original individuals; and (3) the computational costs are lower, since it avoids the efforts to discover the most pure endmembers. Compared with the traditional MESEMA, the locally adaptive MESMA has achieved more accurate and reliable estimations of rocky desertification dynamics in DRR.

With respect to the temporal changes of rocky desertification, we observe an inversed U-shaped trend for desertified land with different severity levels from 1987 and 2013 in DRR. In particular, the inflection point roughly emerged in period 2000–2005. As for the spatial patterns of rocky desertification, the hotspots generally occurred in areas with gentle slope. The casual mechanism-based regressions demonstrate that such dynamics of rocky desertification are closely coupled with socioeconomic, biophysical, and policy factors. We find that road total length positively accounts for area of potential desertified land (severity level 2). This discovery supports the point that intensive but inappropriate human activities play a critical role in transforming land into desertified status (Li et al., 2009; Wu et al., 2011; Xu et al., 2013). It is argued that road construction can significantly increase irrational land use activities (e.g., deforestation, reclamation), which are direct causes of land degradation and desertification (Gao and Liu, 2010). It has been established that poverty is mostly related to land degradation and desertification in tropical countries (Gao and Liu, 2010; Jaquet et al., 2015; Vu et al., 2014a), since poorer communities are more likely to adopt extensive land use practices to pursuit economic gains. My study agree with previous findings, since household income acts as a negative exploratory factor for rocky desertification in DRR. Differently, my results do not confirm previous literature that acknowledges population dynamics as significant contributors to land degradation and desertification (Jaquet et al., 2015; Li et al., 2009; Vu et al., 2014a, 2014b). It should be attributed to the fact that large scale out-immigration has occurred in DRR in recent decades.

Land desertification is widely acknowledged as a result of the combination of biophysical factors and anthropologic activities. Scholars have reported a diversity of biophysical determinants, including topology (Jaquet et al., 2015; Xu et al., 2013), soil types (Yang et al., 2011), lithology (Wang et al., 2004a, 2004b), and geology (Wang et al., 2004a, 2004b). In line with prior cases (Huang and Cai, 2007; Jiang et al., 2009; Xu et al., 2013), my study discovers that slope in particular acts a major biophysical determinant of rocky desertification. Soil depth becomes thinner as slope increases, which raises the difficulty in holding water and soil (Huang and Cai, 2007). In addition, steeper slope limits the labor shortage and maintenance activities (Jaquet et al., 2015). Consequently, areas with steeper slope are more vulnerable to erosion and experience higher possibility of rocky desertification (Xu et al., 2013).

Different from earlier studies that focus on qualitative discussion, this paper evidences the role of policy factors in impacting land desertification using quantitative measurements. More specifically, we identify a significantly positive role of land conservation policy in combating and relieving rocky desertification in DRR. Positive effects are observed particularly through afforestation, investment, and professionals input. Increases in forest coverage as a consequence of the implementation of afforestation plans can directly enhance the ecosystem resilience and reduce the vulnerability to soil erosion. Furthermore, implementation of afforestation plans can also support the socioeconomic improvements (e.g., place attachment, forest-related employment, tourism profit), which are also beneficial for rocky desertification alleviation. The presence of scientific and technological professionals guarantees the effectiveness of land conservation policy. For one thing, it can enhance

Table 2
Outputs of the casual mechanism-based regression (N = 10).

Y	X (standardized coefficient)	R^2
Area of potential desertified land (Severity level 1)	ISTS (-0.131), HI (-0.079), SLOPE (.013)	.45**
Area of potential desertified land (Severity level 2)	TI (-0.386), RTL (.237)	.41**
Total area of potential desertified land	TI (-0.218), HI (-0.052), SLOPE (.029)	.49**
Area of desertified land (Severity level 3)	AA (-0.449), ITD (-0.014), HI (-0.073), SLOPE (.029)	.21**
Area of desertified land (Severity level 4)	AA (-0.305), TI (-0.113), LITH (-0.005)	.54**
Area of desertified land (Severity level 5)	AA (-0.288), TI (-0.245), SLOPE (.018)	.57**
Total area of desertified land	AA (-0.295), ITD (-0.014), HI (-0.225), SLOPE (.031)	.22**

Abbreviations;: afforestation area (AA), involved scientific and technological staff (ISTS), total investment (TI), implementation temporal duration (ITD), road total length (RTL), household income (HI), average slope of non-desertified land (SLOPE), proportion of non-desertified land with lithosol soil type (LITH).
** $p < 0.01$

the trust, partnerships and connections among a range of stakeholders for the smooth execution of related plans and actions. For another, it can ensure that the formulated actions and plans are local-specific and can be implemented practically and appropriately. In this regard, the land conservation policy represents a package of countermeasures that can generate a number of positive eco-environmental and socioeconomic responses to rocky desertification. Interestingly, the implementation temporal duration only accounts for the areal changes of desertified land with severity level 3 but does not contributes to those of desertified land with severity 4 and 5. Two possible factors may explain such discrepancies: (1) the effect of land policy implementation should be nonlinearly cumulative across time; and (2) desertified land with higher severity levels (level 4 and 5) is not easily converted into sustainable land use through afforestation in short time.

6. Policy implications

Orienting rocky desertification towards sustainable land use means that we have to find practical approaches to tackling rocky desertification that develop adaptions that use land use in different ways to enhance ecosystem services and capacity for vegetation recovery and conserve non-desertified land with high ecological value to prevent crossing the critical thresholds for further desertification. The findings of DRR have critical implications for orienting rocky desertification towards sustainable land use. More specifically, the case of DRR highlights that policy-driven afforestation plans should be given pre-requisites for combating rocky desertification. As demonstrated in the DRR case, technical support and knowledge transfer through capital and staff input also contribute towards rocky desertification alleviation. The DRR case also evidences that rocky desertification is determined by various processes and their geographical interlinkages, including socioeconomic, biophysical, and policy aspects. Based on the conclusions and lessons of DRR, I make relevant recommendations as follows for formulating policies and strategies that attempt to orient desertification towards sustainable land use, particularly in the environmentally vulnerable areas where rocky desertification tends to occur.

(1) Adopting active ecological measures to establish local land protective systems. Ecological measures (e.g., plantations of trees and drought-enduring plants) attempts to halt the rocky desertification through restoring the threatened and degraded ecosystems. After suitable mechanical remedies, trees and drought-enduring plants can be planted in the waterlogging-prone areas. It can forms vegetative protection that can prevent the continuous desertification and help reverse the spiral effect into adjacent land. The improved ecosystem services can provide a better environment for the survival of plantations in turn and finally establish local land protection systems.

(2) Fostering sustainable land use investments. Economic incentives (e.g., subsidy) and capital input are promising options to encourage the local stakeholders and households to participate in combating rocky desertification. Rehabilitation engineering of rocky desertification requires a large amount of monetary investment. At current, the central government takes the major responsibility to combat rocky desertification, and consequently acts as the main investor. A conducive environment can be created by the central government to promote investments from the enterprises and investments in the land by the farmers themselves. Such action would support the engineering supply, technical access, absorb productive labor that strengthen the capacity to enlarge the sustainable land use practices.

(3) Designing awareness and knowledge raising schemes. Households are the implement subjects of sustainable land use practices. Improving households' environmental consciousness, knowledge, and skills through training courses and education campaigns should contribute towards increased adaptive capacity to tackle rocky desertification. This recommendation is particularly applicable to the disadvantaged households with less gains from land use and difficulties in obtain skills and knowledge.

(4) Developing advanced and sophisticated tools to guide policies. Biophysical, socioeconomic and policy factors present complex geographical interlinkages in determining rocky desertification. Besides, rocky desertification is not static and the interlinkages among these determinants are likely to change with time. Efforts from the scientific community are urgently needed to develop advanced and sophisticated models and tools to uncover the root mechanisms governing the dynamic rocky desertification, to integrate rocky desertification rehabilitation with national socioeconomic development plans, and to highlight the socioeconomic and biological benefits of combating rocky desertification.

7. Conclusions

This paper proposes a locally adaptive multiple endmember spectral mixture analysis (MESMA) algorithm to extract the rocky desertification information from medium resolution images at subpixel level and applies it to the case of Danjiangkou reservoir region (DRR), China. Quantitative comparisons show that the locally adaptive MESMA has achieved more accurate and reliable estimations of rocky desertification information in DRR than the traditional MESMA. An inversed U-shaped trend is observed for desertified land with different severity levels from 1987 and 2013 in DRR. In particular, the inflection point roughly emerged in period 2000–2005. Casual mechanism-based regressions demonstrate that such dynamics of rocky desertification are closely coupled with socioeconomic, biophysical, and policy factors. More specifically, I identify a significantly positive role of land conservation policy in combating and relieving rocky desertification in DRR. Positive effects are observed particularly through afforestation, investment, and professionals input. Based on the lessons of DRR, I finally make relevant recommendations for formulating policies and strategies that attempt to orient desertification towards

sustainable land use. The proposed locally adaptive MESMA can act as an advanced remote sensing tool to guide the conservation policy. This study also incorporates limitations. First, the used remotely sensed images vary with acquisition time, which should result in bias in rocky desertification estimation. Second, I only estimate the areal information of rocky desertification at sub-pixel level, but fail to obtain the exact location at sub-pixel level. Third, I only consider a listed potential influencing variables given data availability. Last, I focus on the entire DRR and the variations of rocky desertification within the DRR have not been fully examined. Further studies should explore the location of rocky desertification at sub-pixel level and address the bias resulted from multi-temporal data. In particular, the role of land use policy and its interactions with socioeconomic and biophysical factor should be better understood in governing rocky desertification.

Acknowledgement

This research has received financial support by National Natural Science Foundation of China under Grants no. 71403235, by Zhi-Jiang Young Scholar Program of Social Science of Zhejiang Province, under Grant No. 16ZJQN026YB and by Zhejiang Provincial Natural Science Foundation of China under Grant no. LQ14G030016.

Appendix A.

Description of remotely sensed data sources.

No.	Acquisition time	Sensor	Average cloud (%)	Path/Row
1	1987.10.26	Landsat 5	0.0	125/37, 125/38
2	1996.10.18	Landsat 5	2.5	125/37, 125/38
3	2001.9.30	Landsat 5	2.7	125/37, 125/38
4	2002.9.25	Landsat 7	1.7	125/37, 125/38
5	2004.10.08	Landsat 5	0.3	125/37, 125/38
6	2007.9.15	Landsat 5	0.0	125/37, 125/38
7	2008.5.1	CBERS 2	0.0	4/63, 4/64
8	2010.5.2	Landsat 5	0.0	125/37, 125/38
9	2011.7.8	Landsat 5	0.8	125/37, 125/38
10	2013.8.14	Landsat 8	2.3	125/37, 125/38

Appendix B.

Official standard of rocky desertification severity classification in Hubei Province, China.

	Vegetation%	Bedrock%	Severity level
Potential desertification	<50	30–40	1
	<50	40–50	2
Desertification	<50	50–70	3
	<50	70–80	4
	<50	>80	5

References

Achard, F., Eva, H.D., Stibig, H.-J., Mayaux, P., Gallego, J., Richards, T., et al., 2002. Determination of deforestation rates of the world's humid tropical forests. Science 297, 999–1002.
Asner, G.P., Lobell, D.B., 2000. A biogeophysical approach for automated SWIR unmixing of soils and vegetation. Remote Sens. Environ. 74, 99–112.
Aubréville, A., 1949. Climats, forêts et desertification de l'Afrique tropicale. Société D'Editions Géographiques, Maritimes et Coloniales: Paris, France.
Bai, Z., Dent, D., Olsson, L., Schaepman, M., 2008. Proxy global assessment of land degradation. Soil Use Manage. 24, 223–234.
Bai, X., Wang, S., Xiong, K., 2013. Assessing spatial-temporal evolution processes of karst rocky desertification land: indications for restoration strategies. Land Degrad. Dev. 24, 47–56.
Bastin, G.N., Pickup, G., Pearce, G., 1995. Utility of AVHRR data for land degradation assessment: a case study. Int. J. Remote Sens. 16, 651–672.
Bateson, C.A., Asner, G.P., Wessman, C.A., 2000. Endmember bundles: a new approach to incorporating endmember variability into spectral mixture analysis. IEEE Trans. Geosci. Remote Sens. 38, 1083–1094.
Bot, A.J., Nachtergaele, F.O., Young, A., 2000. Land Resource Potential and Constraints at Regional and Country Levels. Food and Agriculture Organization of the United Nations, Rome (L. a. W. D. Division, Trans.).
Bruce, V., Green, P.R., Georgeson, M.A., 2003. Visual Perception: Physiology, Psychology, & Ecology, 4th edn. Psychology Press, Hove & London.
Cai, X., Zhang, X., Wang, D., 2011. Land availability for biofuel production. Environ. Sci. Technol. 45, 334–339.
Campbell, J.E., Lobell, D.B., Genova, R.C., Field, C.B., 2008. The global potential of bioenergy on abandoned agriculture lands. Environ. Sci. Technol. 42, 5791–5794.
Campbell, J.B., 2002. Introduction to Remote Sensing, 3rd edn. Guilford Press, New York, NY.
Chen, Q., Lan, A., Xiong, K., Xiao, S., Wang, J., Xiong, J., 2003. Spectral feature-based model for extracting karst rock-desertification from remote sensing image. J. Guizhou Normal Univ. (Nat. Sci.) 21, 82–87 (in Chinese with English abstract).
Dawelbait, M., Morari, F., 2012. Monitoring desertification in a Savannah region in Sudan using Landsat images and spectral mixture analysis. J. Arid Environ. 80, 45–55.
Dean, W.R.J., Hoffman, M.T., Meadows, M.E., Milton, S.J., 1995. Desertification in the semi-arid Karoo, South Africa: review and reassessment. J. Arid Environ. 30, 247–264.
Deng, C., Wu, C., 2013. A spatially adaptive spectral mixture analysis for mapping subpixel urban impervious surface distribution. Remote Sens. Environ. 133, 62–70.
Dennison, P.E., Roberts, D.A., 2003. Endmember selection for multiple endmember spectral mixture analysis using endmember average RSME. Remote Sens. Environ. 87, 123–135.
Dimobe, K., Ouédraogo, A., Soma, S., Goetze, D., Porembski, S., Thiombiano, A., 2015. Identification of driving factors of land degradation and deforestation in the wildlife reserve of Bontioli (Burkina Faso, West Africa). Glob. Ecol. Conserv. 4, 559–571.
ELD Initiative, 2013. The Rewards of Investing in Sustainable Land Management. Interim Report for the Economics of Land Degradation Initiative: A global strategy for sustainable land management. Available from: www.eld-initiative.org.
FAO (Food and Agriculture Organization), 1979. A Provisional Methodology for Soil Degradation Assessment. UN Food and Agriculture Organization, Rome.
FAO (Food and Agriculture Organization), 2001. Global forest resources assessment 2000. FAO For. Pap. 140, 479.
Fleskens, L., Stringer, L.C., 2014. Land management and policy responses to mitigate desertification and land degradation. Land Degrad. Dev. 25, 1–4.
Ford, D., Williams, P., 2007. Karst Hydrogeology and Geomorphology. John Wiley & Sons Ltd, England.
Franke, J., Roberts, D.A., Halligan, K., Menz, G., 2009. Hierarchical multiple endmember spectral mixture analysis (MESMA) of hyperspectral imagery for urban environments. Remote Sens. Environ. 113, 1712–1723.
Gams, I., Gabrovec, M., 1999. Land use and human impact in the Dinaric Karst. Int. J. Speleol. 28 B, 55–70.
Gao, J., Liu, Y., 2010. Determination of land degradation causes in Tongyu County: northeast China via land cover change detection. Int. J. Appl. Earth Obs. Geoinf. 12, 9–16.
García, M., Oyonarte, C., Villagarcía, L., Contreras, S., Domingo, F., Puigdefábregas, J., 2008. Monitoring land degradation risk using ASTER data: the non-evaporative fraction as an indicator of ecosystem function. Remote Sens. Environ. 112, 3720–3736.
Geist, H.J., Lambin, E.F., 2004. Dynamic causal patterns of desertification. BioScience 54, 817–829.
Gibbs, H.K., Salmon, J.M., 2015. Mapping the world's degraded lands. Appl. Geogr. 57, 12–21.
Glantz, M.H., Orlovsky, N.S., 1983. Desertification: a review of the concept. Desertification Control Bull. 9, 15–22.
Grainger, A., 2009. The role of science in implementing international environmental agreements: the case of desertification. Land Degrad. Dev. 20, 410–430.
Hartia, A., Lhissou, R., Chokmani, K., Ouzemou, M., Hassouna, J., Bachaoui, M., Ghmar, A., 2016. Spatiotemporal monitoring of soil salinization in irrigated Tadla Plain (Morocco) using satellite spectral indices. Int. J. Appl. Earth Obs. Geoinf. 50, 64–73.
Herrmann, S.M., Hutchinson, C.F., 2005. The changing contexts of the desertification debate. J. Arid Environ. 63, 538–555.
Hill, J., Méıgier, J., Mehl, W., 1995. Land degradation: soil erosion and desertification monitoring in Mediterranean ecosystems. Remote Sens. Rev. 12, 107–130.
Huang, Q., Cai, Y., 2007. Spatial pattern of Karst rock desertification in the Middle of Guizhou Province: Southwestern China. Environ. Geol. 52, 1325–1330.
IPCC (International Panel of Climate Change), 2001. Climate Change 2001: Impacts, Adaptation, and Vulnerability. Cambridge University Press, Cambridge.
Jackson, D.C., 1960. Erosion control research in the Central African Federation. Q. Rev. Cent. Afr. Assoc. Med. Lab. Technol. 3, 61–70.
Jaquet, S., Schwilch, G., Hartung-Hofmann, F., Adhikari, A., Sudmeier-Rieux, K., Shrestha, G., et al., 2015. Does outmigration lead to land degradation? Labour shortage and land management in a western Nepal watershed. Appl. Geogr. 62, 157–170.

Jiang, Y., Li, L., Groves, C., Yuan, D., Kambesis, P., 2009. Relationships between rocky desertification and spatial pattern of land use in typical karst area: southwest China. Environ. Earth Sci. 59, 881–890.
Jiang, Z., Lian, Y., Qin, X., 2014. Rocky desertification in Southwest China: impacts causes, and restoration. Earth Sci. Rev. 132, 1–12.
Kasperson, J., Kasperson, R., Turner, B., 1995. Regions at Risk. United Nations University Press (http://www.unu.edu/unupress/unupbooks/uu14re/uu14re00. htm).
Kiage, L.M., 2013. Perspectives on the assumed causes of land degradation in the rangelands of Sub-Saharan Africa. Prog. Phys. Geogr. 37, 664–684.
Lal, R., 1977. Review of soil erosion research in Latin America. In: Greenland, D.J., Lal, R. (Eds.), Soil Conservation and Management in the Humid Tropics. John Wiley & Sons, NY, pp. 231–240.
Lamchin, M., Lee, J., Lee, W., Lee, E., Kim, M., Lim, C., Choi, H., Kim, S., 2016. Assessment of land cover change and desertification using remote sensing technology in a local region of Mongolia. Adv. Space Res. 57, 64–77.
Lepers, E., Lambin, E.F., Janetos, A.C., DeFries, R., Achard, F., Ramankutty, N., et al., 2005. A synthesis of information on rapid land-cover change for the period 1981–2000. BioScience 55, 115–124.
Li, Y., Shao, J., Yang, H., Bai, X., 2009. The relations between land use and karst rocky desertification in a typical karst area, China. Environ. Geol. 57, 621–627.
Liu, Y., Feng, Y., Zhao, Z., Zhang, Q., Su, S., 2016. Socioeconomic drivers of forest loss and fragmentation: a comparison between different land use planning schemes and policy implications. Land Use Policy 54, 58–68.
MAGRAMA, 2008. Programa de Acción Nacional contra la Desertificación. Madrid. 262 p. http://www.unccd.int/ActionProgrammes/spain-spa2008. pdf.
MEA (Millennium Ecosystem Assessment), 2005. Ecosystems and Human Well-being: Synthesis. Island Press, Washington D.C.
Ma, B., Wu, L., Zhang, X., Li, X., Liu, Y., Wang, S., 2014. Locally adaptive unmixing method for lake-water area extraction based on MODIS 250 m bands. Int. J. Appl. Earth Obs. Geoinf. 33, 109–118.
Miao, L., Moore, J.C., Zeng, F., Lei, J., Ding, J., He, B., Cui, X., 2015. Footprint of research in desertification management in China. Land Degrad. Dev. 26, 450–457.
NAP, 2002. Vietnam National Action Programme to Combat Desertification, Vietnam NAP for UNCCD Implementation. http://www.unccd.int/ActionProgrammes/vietnam-eng2002.pdf.
Nijsen, M., Smeets, E., Stehfest, E., Vuuren, D.P., 2012. An evaluation of the global potential of bioenergy production on degraded lands. GCB Bioenergy 4, 130–147.
Nkonya, E., Gerber, N., Baumgartner, P., von Braun, J., De Pinto, A., Graw, V., Kato, E., Kloos, J., Walter, T., 2011. The Economics of Land Degradation: Toward An Integrated Global Assessment. Peter Lang, Frankfurt am Mainz.
Pan, J., Qin, X., 2010. Extracting desertification from Landsat imagery using a feature space composed of vegetation index and albedo —a case study of Zhangye oasis and its adjacent areas. Surv. Mapp. Sci. 3, 193–195.
Pender, J., Mirzabaev, A., 2008. Economic analysis of sustainable land management options in central Asia, [progress report] (ADB).
Piao, S., Fang, J., Liu, H., Zhu, B., 2005. NDVI-indicated decline in desertification in China in the past two decades. Geophys. Res. Lett. 32, L06402.
Prince, S.D., Becker-Reshef, I., Rishmawi, K., 2009. Detection and mapping of long-term land degradation using local net production scaling: application to Zimbabwe. Remote Sens. Environ. 113, 1046–1057.
Qi, Y., Chang, Q., Jia, K., Liu, M., Liu, J., Chen, T., 2012. Temporal-spatial variability of desertification in an agro-pastoral transitional zone of northern Shaanxi Province. China Catena 88, 37–45.
Ramankutty, N., Foley, J.A., 1999. Estimating historical changes in global land cover: croplands from 1700 to 1992. Glob. Biogeochem. Cycles 13, 997–1027.
Rashed, T., Weeks, J.R., Roberts, D., Rogan, J., Powell, R., 2003. Measuring the physical composition of urban morphology using multiple endmember spectral mixture models. Photogramm. Eng. Remote Sens. 69, 1011–1020.
Reynolds, J.F., Smith, D.M.S., Lambin, E.F., Turner, B.L., Mortimore, M., Batterbury, S.P.J., et al., 2007. Global desertification: building a science for dryland development. Science 316, 847–851.
Roberts, D.A., Gardner, M., Church, R., Ustin, S., Scheer, G., Green, R.O., 1998. Mapping chaparral in the Santa Monica Mountains using multiple endmember spectral mixture models. Remote Sens. Environ. 65, 267–279.
SFA (State Forestry Administration), 2004. Six key forestry programs: rebuild beautiful mountains of the great pioneering actions in China. Beijing.
Safriel, U., Adeel, Z., 2005. Chapter 22. Dryland systems. In: Hassan, R., Scholes, R.J., Ash, N. (Eds.), Ecosystems and Human Well-being: Current State and Trends, Vol. 1. Island Press, London, p. 917.
Salvati, L., Bajocco, S., 2011. Land sensitivity to desertification across Italy: past present, and future. Appl. Geogr. 31, 223–231.
Saygın, S.D., Basaran, M., Ozcan, A.U., Dolarslan, M., Timur, O.B., Yilman, E.F., Erpul, G., 2011. Land degradation assessment by geo-spatially modeling different soil erodibility equations in a semi-arid catchment. Environ. Monit. Assess. 180, 201–215.
Shi, C., Wang, L., 2014. Incorporating spatial information in spectral unmixing: a review. Remote Sens. Environ. 149, 70–87.
Somers, B., Asner, G.P., Tits, L., Coppin, P., 2011. Endmember variability in spectral mixture analysis: a review. Remote Sens. Environ. 115, 1603–1616.
Somers, B., Zortea, M., Plaza, A., Asner, G.P., 2012. Automated extraction of image-based endmember bundles for improved spectral unmixing. IEEE J. Sel. Top. Appl. Earth Obs. Remote Sens. 5, 396–408.
Song, C., 2005. Spectral mixture analysis for subpixel vegetation fractions in the urban environment: how to incorporated endmember variability. Remote Sens. Environ. 95, 248–263.
Stringer, L.C., 2009. Testing the orthodoxies of land degradation policy in Swaziland. Land Use Policy 26, 157–168.
Su, S., Jiang, Z., Zhang, Q., Zhang, Y., 2011. Transformation of agricultural landscapes under rapid urbanization: a threat to sustainability in Hang-Jia-Hu region, China. Appl. Geogr. 31, 439–449.
Su, S., Zhang, Z., Xiao, R., Jiang, Z., Chen, T., Zhang, L., et al., 2012. Geospatial assessment of agroecosystem health: development of an integrated index based on catastrophe theory. Stochastic Environ. Res. Risk Assess. 26, 321–334.
Su, S., Yang, C., Hu, Y., Luo, F., Wang, Y., 2014. Progressive landscape fragmentation in relation to cash crop cultivation. Appl. Geogr. 53, 20–31.
Su, S., Zhou, X., Wan, C., Li, Y., Kong, W., 2016. Land use changes to cash crop plantations: crop types: multilevel determinants and policy implications. Land Use Policy 50, 379–389.
Sun, D., 2015. Detection of dryland degradation using Landsat spectral unmixing remote sensing with syndrome concept in Minqin County: China. Int. J. Appl. Earth Obs. Geoinf. 41, 34–45.
Sunkar, A., 2008. Deforestation and rocky desertification processes in Gunung Sewu karst landscape. Media Konservasi 13, 1–7.
Symeonakis, E., Drake, N., 2004. Monitoring desertification and land degradation over sub-Saharan Africa. Int. J. Remote Sens. 25, 573–592.
Thomas, D.S.G., Middleton, N.J., 1994. Desertification: Exploding The Myth. John Wiley & Sons Ltd, Chichester, UK, ISBN 0–471-94815–2.
Thomas, R.J., Akhtar-Schuster, M., Stringer, L.C., Marques, M.J., Escadafal, R., Abraham, E., Enne, G., 2012. Fertile ground?: Options for a science-policy platform for land. Environ. Sci. Policy 16, 122–135.
Trimble, S.W., 1985. Perspectives of the history of soil erosion control in the eastern United States. In: Helms, D., Flader, S. (Eds.), The History of Soil and Water Conservation. Agricultural History Society, Washington, DC, pp. 60–78.
Tromp, M., Epema, G.F., 1999. Spectral mixture analysis for mapping land degradation in semi-arid areas. Netherlands J. Geosci. Geol. En Mijnb. 77, 153–160.
UNCCD (United Nations Convention to Combat Desertification), 1994. United Nations Convention to Combat Desertification in Those Countries Experiencing Serious Drought And/or Desertification Particularly in Africa: Text with Annexes. UNEP, Nairobi.
UNCCD (United Nations Convention to Combat Desertification), 1995. Convención de las Naciones Unidas de Lucha contra la Desertificación en los países afectados por sequía grave o Desertificación, en particular en África. Texto con Anexos, Documento Oficial de la UNCCD.
UNCCD (United Nations Convention to Combat Desertification), 2008. Desertification-coping with today's global challenges in the context of the strategy of the UNCCD.
UNEP, 1997. In: Middleton, N., Thomas, D.S.G. (Eds.), World Atlas of Desertification. , second ed. Edward Arnold, London.
Vägen, T.G., Winowiecki, L.A., Abegaz, A., Hadgu, K.M., 2013. Landsat-based approaches for mapping of land degradation prevalence and soil functional properties in Ethiopia. Remote Sens. Environ. 134, 266–275.
Verstraete, M.M., 1986. Defining desertification: a review. Clim. Change 9, 5–18.
Vieira, R.M.S.P., Tomasella, J., Alvalá, R.C.S., Sestini, M.F., Affonso, A.G., Rodriguez, D.A., et al., 2015. Identifying areas susceptible to desertification in the Brazilian northeast. Solid Earth 6, 347–360.
Vlek, P.L.G., Le, Q.B., Tamene, L., 2008. Land Decline in Land-Rich Africa: A Creeping Disaster in the Making. CGIAR Science Council Secretariat, Rome, Italy.
Vogt, J.V., Safriel, U., Von Maltitz, G., Sokona, Y., Zougmore, R., Bastin, G., Hill, J., 2011. Monitoring and assessment of land degradation and desertification: towards new conceptual and integrated approaches. Land Degrad. Dev. 22, 150–165.
Vu, Q.M., Le, Q., Vlek, P.L.G., 2014a. Hotspots of human-induced biomass productivity decline and their social-ecological types toward supporting national policy and local studies on combating land degradation. Glob. Planet. Change 121, 64–77.
Vu, Q.M., Le, Q., Frossard, E., Vlek, P.L.G., 2014b. Socio-economic and biophysical determinants of land degradation in Vietnam: an integrated causal analysis at the national level. Land Use Policy 36, 605–617.
Wan, C., Su, S., 2016. 2016 Neighborhood housing deprivation and public health: theoretical linkage, empirical evidence, and implications for urban planning. Habitat Int. 57, 11–23.
Wang, T., Wu, W., Xue, X., 2004a. Temporal and spatial changes of desertified land in Northern China in the past 50 years. Acta Geog. Sin. 59, 203–212.
Wang, S., Liu, Q., Zhang, D., 2004b. Karst rocky desertification in southwestern China: geomorphology land use, impact and rehabilitation. Land Degrad. Dev. 15, 115–121.
Wang, X., Chen, F., Hasi, E., Li, J., 2008. Desertification in China: an assessment. Earth Sci. Rev. 88, 188–206.
Wessels, K.J., van den Bergh, F., Scholes, R.J., 2012. Limits to detectability of land degradation by trend analysis of vegetation index data. Remote Sens. Environ. 125, 10–22.
Williams, M., 2015. Earth air, fire and water: distinguishing human impacts from natural desertification in SouthAustralia. Trans. R. So. S. Aust. 139, 9–18.
Wolfgramm, B., Stevenson, S., Lerman, Z., Zähringer, J., Liniger, H., 2011. PPCR component A5, phase 1: agriculture & sustainable land management. Final report prepared for the World Bank.

https://www.wocat.net/en/news-events/global-news/newsdetail/article/final-report-of-the-pilotprogram-for-climate-resilience-ppcr.html.
Wu, J., Liu, Y., Wang, J., He, T., 2010. Application of Hyperion data to land degradation mapping in the Hengshan region of China. Int. J. Remote Sens. 31, 5145–5161.
Wu, X., Liu, H., Huang, X., Zhou, T., 2011. Human driving forces: analysis of rocky desertification in karst region in Guanling County: Guizhou Province. Chin. Geog. Sci. 21, 600–608.
Xiao, J., Shen, Y., Tateishi, R., et al., 2006. Development of topsoil grain size index for monitoring desertification in arid land using remote sensing. Int. J. Remote Sens. 27, 2411–2422.
Xiao, R., Su, S., Mai, G., Zhang, Z., Yang, C., 2015. Quantifying determinants of cash crop expansion and their relative effects using logistic regression modeling and variance partitioning. Int. J. Appl. Earth Obs. Geoinf. 34, 258–263.
Xiong, Y., Qiu, G., Mo, D., Lin, H., Sun, H., Wang, Q., Zhao, S., Yin, J., 2008. Rocky desertification and its causes in karst areas: a case study in Yongshun County Hunan Province, China. Environ. Geol. 57, 1481–1488.
Xu, E., Zhang, H., Li, M., 2013. Mining spatial information to investigate the evolution of karst rocky desertification and its human driving forces in Changshun, China. Sci. Total Environ. 458–460, 419–426.
Xu, E., Zhang, H., Li, M., 2015. Object-based mapping of karst rocky desertification using a support vector machine. Land Degrad. Dev. 26, 158–167.
Xue, X., Wang, T., Wu, W., 2005. The desertification development and its causes of agro-pastoral mixed regions in North China. J. Desert Res. 25, 320–328.
Yan, X., Cai, Y.L., 2015. Multi-scale anthropogenic driving forces of Karst Rocky Desertification in Southwest China. Land Degrad. Dev. 26, 193–200.
Yang, Q., Wang, K., Zhang, C., Yue, Y., Tian, R., Fan, F., 2011. Spatio-temporal evolution of rocky desertification and its driving forces in karst areas of Northwestern Guangxi, China. Environ. Earth Sci. 64, 383–393.
Yassoglou, N., 2000. History of desertification in the European Mediterranean. In: Enne, G., D'Angelo, M., Zanolla, C. (Eds.), Indicators for Assessing Desertification in the Mediterranean. Proceedings of the International Seminar Held in Porto Torres, Italy, 18–20 September, 1998. University of Sassari Nucleo Ricerca Desertificazion, Sassari, Italy, pp. 9–15.
You, H., 2016. Characterizing the inequalities in urban public green space provision in Shenzhen, China. Habitat Int. 56, 176–180.
Yuan, D.X., 1997. Rock desertification in the subtropical karst of south China. Z Geomorphol 108, 81–90.
Yue, Y., Zhang, B., Wang, K., Li, R., Liu, B., Zhang, M., 2011. Remote sensing of indicators for evaluating karst rocky desertification. J. Remote Sens. 15, 722–736.
Zare, A., Gader, P., 2010. PCE: Piece-wise convex endmember detection. IEEE Trans. Geosci. Remote Sens. 48, 2620–2632.
Zhang, X., Shang, K., Cen, Y., Shuai, T., Sun, Y., 2014. Estimating ecological indicators of karst rocky desertification bylinear spectral unmixing method. Int. J. Appl. Earth Obs. Geoinf. 31, 86–94.
Zhao, X., Luo, Y., Wang, S., Huang, W.D., Lian, J., 2010. Is desertification reversion sustainable in Northern China? A case study in Naiman County, part of a typical agro-pastoral transitional zone in Inner-Mongolia, China. Glob. Environ. Res. 14, 63–70.
Zhao, X., Wu, P., Gao, X., Persaud, N., 2015. Soil quality indicators in relation to land use and topography in a small catchment on the Loess Plateau of China. Land Degrad. Dev. 26, 54–61.
Zhou, L., Zhu, Y., Huang, Y., 2012. Quantitative evaluation of the effect of prohibiting grazing on restoration of desertified grassland in agro-pastoral transitional zone in Northern China. J. Desert Res. 32, 308–313.
Zhu, Z., Wang, T., 1993. Trends of desertification and its rehabilitation. Desertification Bull. 22, 27–30.
von Braun, J., Gerber, N., Mirzabaev, A., Nkonya, E., 2012. The Economic of Land Degradation –An Issue Paper, Global Soil Week 2012. Global Soil Forum, Institute for Advanced Sustainability Studies, Postdam, pp. 1–30.